

Spatially Indirect Exciton Condensation in Two-Dimensional Strongly Correlated Semimetals

Yao Zeng, Shi-Cong Mo, Xiang Chen, and Wéi Wú*

*Guangdong Provincial Key Laboratory of Magnetoelectric Physics and Devices and
School of Physics, Sun Yat-sen University, Guangzhou, Guangdong 510275, China*

(Dated: June 19, 2026)

Identifying materials hosting an excitonic insulator ground state has been one of the major pursuits in condensed matter physics in recent years. Promising candidates in transition metal chalcogenide compounds (TMC), including $1T$ -TiSe₂, Ta₂Pd₃Te₅, and Ta₂NiSe₅, share a crucial common characteristic: their low-energy physics is governed by electrons in d -orbitals subject to strong on-site Coulomb interactions. In this work, we investigate spatially indirect exciton condensation in two-dimensional semimetals on triangular lattice. Using a combination of dynamical mean-field theory and the determinant quantum Monte Carlo method, we study two- and three-orbital Hubbard models incorporating strong on-site (U) and inter-orbital interactions (V). Our results demonstrate that on-site Hubbard U can strongly suppress the condensation temperature T_c , an effect that is particularly pronounced at higher electron-hole pair densities. This behavior contrasts sharply with the case without on-site U , where T_c grows with pair density at fixed V . Moreover, we uncover competition among multiple electron-hole pairing channels in the three-orbital model, which also acts to suppress T_c of exciton condensation. An orbital-selective electron-hole pairing state is identified. These findings may help explain the large discrepancy between strong binding-energy and relative low transition temperature for indirect excitons in TMCs materials, offering important insights for understanding and engineering exciton condensation in materials with strongly correlated d -shell electrons.

Introduction - The excitonic insulator (EI) constitutes a paradigmatic correlated state arising from a bosonic condensation of Coulomb-bound electron-hole pairs in narrow-gap semiconductors or semimetals [1–4]. This fundamental phase of matter has been investigated extensively in both experiment [5–15] and theory [2, 3, 6, 16–23]. The spatially separated electron-hole bilayer structures [4] provide particularly favorable platforms for achieving this state, as spatial separation suppresses electron-hole recombination, hence prolonging exciton lifetimes and promotes the condensation of indirect excitons. The exploration of many exotic emergent phenomena related to EI, such as the BCS-BEC crossover [24–32], supersolidity [33–35], finite momentum pairing [36–39], excitonic topological phases [11, 40], and perfect Coulomb drag [41, 42], can thus be facilitated in the indirect exciton systems.

Quantum wells in InAs/GaSb heterostructures have served as pioneering platforms in the pursuit of these exotic phases [40, 43]. These semiconductor systems revealed signatures of excitonic topological order and superfluidity [4, 40, 44]. More recently, transition metal chalcogenide (TMC) platforms, such as MoSe₂/hBN/WSe₂ heterostructures, have been pivotal systems for exploring high-temperature EI [41, 42]. By exploiting Type-II band alignment to spatially separate carriers, these devices host long-lived excitons that exhibit macroscopic coherence, evidenced by nonlinear electroluminescence up to 100 K [32]. Crucially, transport measurements revealed perfect Coulomb drag at zero magnetic field [41, 42], establishing a key foundation for realizing frictionless flow of charge-neutral exci-

tions [45–48] in transport experiments. In bulk EI materials, on the other hand, the layered TMC compounds $1T$ -TiSe₂ [5, 49–51], Ta₂Pd₃Te₅ [9, 10], and Ta₂NiSe₅ [9, 10, 21, 52–55] have sparked intense debate regarding the existence of exciton condensation. This is because the gap opening in these materials, a hallmark of the excitonic ordered state, can also be attributed to non-excitonic structure phase transitions [8, 56–59]. Compared to Ta₂NiSe₅, which may host significant structural distortion [58, 60], Ta₂Pd₃Te₅ offers a cleaner paradigm, as in which the lattice distortion is negligible in the insulating phase [9, 10]. This structural stability strongly supports an exciton instability driven by Coulomb interactions in Ta₂Pd₃Te₅.

While experimental advances in the study of EI have progressed rapidly, a comprehensive theoretical understanding [17, 24, 35, 61–65] of this phase in real materials remains incomplete. We notice that in theory, large exciton binding energies being order of ~ 1 eV have been predicted in semi-metals or narrow gap semiconductors [21, 66–68], a high temperature EI in experiments, however, is still elusive. Conventional theoretical frameworks are often established on the basis of mean-field or perturbative approaches. In EI candidate materials based on TMC, the strong on-site Hubbard interaction U in d -orbitals is usually larger than the electron bandwidth W [69], and it can significantly exceed the inter-orbital (inter-layer) electron-hole attraction V [56]. This strong-correlation regime calls into question the adequacy of weak-coupling theories that consider V while neglecting the substantial on-site interaction U .

In this work, we investigate excitonic condensation in

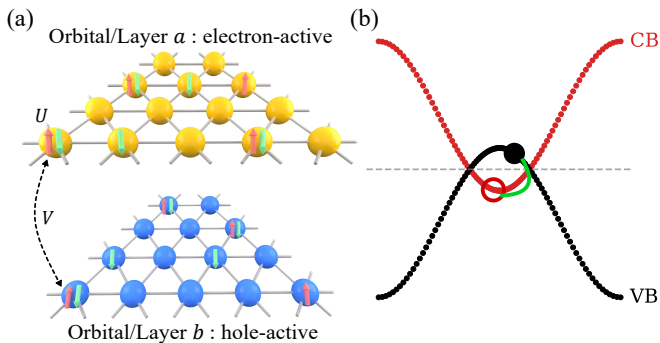


FIG. 1. **(a)** Schematic illustration of the two-orbital (two-layer) Hubbard model on 2D triangular lattice. U represents the on-site intra-orbital (intra-layer) Coulomb interaction, while V denotes the inter-orbital (inter-layer) Coulomb interaction in a unit cell. The orbital/layer a (upper) is designated as electron-active, while orbital/layer b (lower) acts as hole-active. Dotted line indicates a possible electron-hole pairing. **(b)** Schematic illustration of the non-interacting band structure we use which is a semimetal at $U = 0, V = 0$. Upper/lower curves indicate the conduction/valence bands (CB/VB). The binding of holes at the CB bottom (hollow circles) and electrons at the VB top (filled circles) leads to the formation of indirect excitons (indicated by the solid line between the two circles). Dashed line indicates the Fermi level.

two-dimensional (2D) semimetals using a combination of Cellular dynamical Mean-Field theory (CDMFT) [70] and determinant quantum Monte Carlo (DQMC) [71]. The non-perturbative CDMFT approach enables us to capture the quantum fluctuation of strongly interacting d - electrons beyond weak-coupling treatments. We show that the exciton condensation temperature T_c can be significantly suppressed by on-site Coulomb repulsion U , although it in general remains non-zero for finite V . We also show that a finite U fundamentally modifies the density dependence of T_c . Specifically, T_c drops with increasing carrier concentration n , which contrasts with the $U = 0$ case, where T_c grows with pair density n at fixed V . Using a three-orbital model, we further uncover the competition between different pairing channels, which provides an additional mechanism suppressing T_c . An orbital-selective EI state is also revealed in this model. Finally, we discuss the implications of these findings for experimental observations.

Model and Methods - Our two-orbital Hubbard model we use is given by,

$$H = - \sum_{\langle ij \rangle \sigma m} t_m c_{i\sigma m}^\dagger c_{j\sigma m} + \text{H.c.} - \sum_{i\sigma m} (\mu - \epsilon_m) \hat{n}_{i\sigma m} + \sum_{im} U_m \hat{n}_{i\uparrow m} \hat{n}_{i\downarrow m} + V \sum_{i\sigma\sigma', m \neq m'} \hat{n}_{i\sigma m} \hat{n}_{i\sigma' m'} \quad (1)$$

where the $m = a, b$ labels the orbital (or layer) degrees of freedom, corresponding to orbitals in bulk systems and layers in 2D materials, respectively. $c_{i\sigma m}$ ($c_{i\sigma m}^\dagger$) denotes

the electron annihilation (creation) operator at unit cell i , orbital (layer) m , with spin σ ; $n_{i\sigma m}$ is the particle number operator. The nearest-neighbor hopping integral t_a is set to $t_a = t = 1$ as energy unit throughout the paper. U_m is the on-site repulsion between electrons at orbital (layer) $-m$, V is the local inter-orbital (inter-layer) interaction. In this work, we have omitted long-range Coulomb interactions to simplify the numerical study. We adjust chemical potential μ and orbital(layer) energy ϵ_m to tune the orbital (layer) densities. Here we adopt a pure electron picture to study the problem, *i.e.*, $\langle \hat{n}_a \rangle = n_e \equiv n$ denote the carrier density in the electron orbital (orbital- a), implying a hole orbital (layer) of $n_h = 1 - \langle \hat{n}_b \rangle = n_e = n$ in the orbital- b . We assume equal mass for both carriers, *i.e.*, $t_a = -t_b$. The schematic of our model and the simplified semimetal band structure are illustrated in Fig. 1. Orbitals (layers) a (upper) and b (lower) are designated as electron-active and hole-active, respectively. Previous studies have used the two-orbital Hubbard model to investigate excitonic effects in the strongly correlated regime [72], such as the transition between excitonic insulator state and antiferromagnetic state [73], as well as the interplay between the excitonic insulator and low-/high-spin states [74].

Our theoretical investigation of the bilayer Hubbard model on a triangular lattice is carried out by the Cellular Dynamical Mean-Field Theory, a cluster extension of CDMFT [70] designed to incorporate non-local spatial correlations. In this framework, the lattice problem is mapped onto an effective quantum impurity model for a small cluster, which is then solved self-consistently within a dynamical bath that represents the rest of the lattice degrees of freedom. Here we typically use a two-site effective cluster incorporating a, b orbitals within a unit cell. The effective cluster problem is solved using the continuous-time quantum Monte Carlo method (CTQMC)[75, 76]. Our simulations typically accumulate 10^9 Monte Carlo sweeps in each CDMFT loop. Additional details on the numerical method can be found in the Supplementary Information.

Result - The onset of the excitonic condensation phase can be identified by the divergence of the uniform excitonic pairing susceptibility χ , which can be defined as,

$$\chi = \frac{1}{N} \sum_{i,j} \int_0^\beta d\tau \langle \mathcal{T}_\tau p_j(\tau) p_i(0) \rangle \quad (2)$$

where p_i is the uniform spin-singlet electron-hole pair operator [25], $p_i = \frac{1}{\sqrt{2}} \sum_\sigma \langle c_{ia\sigma}^\dagger c_{ib\sigma} \rangle$, and N is the number of unit cells in the system. Thus the vanishing inverse pairing susceptibility $1/\chi \rightarrow 0$ can be used to determine the critical transition temperature T_c for excitonic condensation (*i.e.*, T_c for EI). We note that in our study, spin-singlet and spin-triplet excitons are degenerated in energy due to the symmetry of our Hamiltonian in Eq.1. In real materials, the energy difference

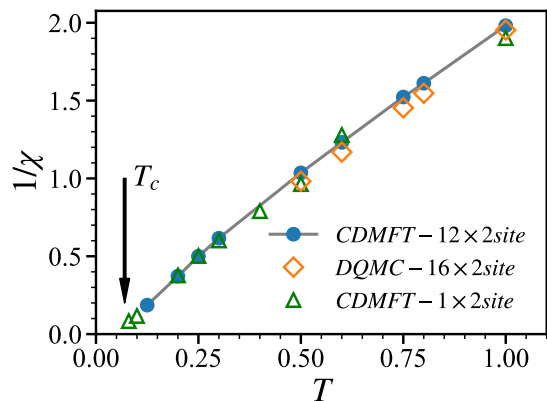


FIG. 2. The inverse susceptibility $1/\chi$ as a function of temperature T . When $1/\chi$ approaches zero, the system enters the excitonic condensate phase, and the corresponding temperature is defined as the critical transition temperature T_c . Here, $U_a = U_b = 1$, $V = 4$, density, $\langle n_a \rangle = 0.2$, $\langle n_b \rangle = 0.8$ (thus $n_e = n_h = 0.2$). An excitonic condensation T_c is found about $T_c \sim 0.07$. The DQMC calculations were performed on a $4 \times 4 \times 2$ lattice, while CDMFT calculations were performed on 1×2 - and 12×2 -site clusters.

between singlet and triplet interlayer excitons may depend on detailed material properties [77–79]. In Fig. 2, we plot the CDMFT result of $1/\chi$ as a function of temperature T for a typical parameter set: $U_a = U_b = 1$, $V = 4$, and electron-hole density $n = 0.2$. As the temperature decreases from $T = 1.0$ to $T = 0.1$, $1/\chi$ drops monotonically from $1/\chi \approx 2.0$ to $1/\chi \approx 0.1$, signaling a growing tendency to El condensation as T reduces. As T approaches $T_c \approx 0.07$, $1/\chi$ vanishes, denoting an El instability in the system at the given parameters. We observe excellent agreement of 1×2 - and 12×2 - site CDMFT with exact high- T DQMC results on a $4 \times 4 \times 2$ - site lattice, thereby justifying the use of CDMFT to

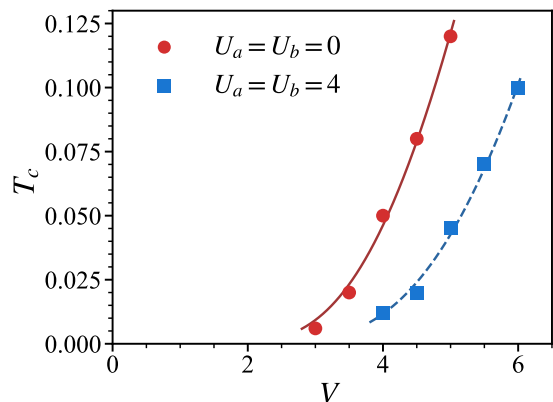


FIG. 3. Transition temperature T_c as a function of the inter-orbital interaction V at different on-site interactions $U_a = U_b \equiv U$. Here, electron-hole density is fixed at $n_e = n_h = 0.06$, data points show results for $U = 0$ (dots) and $U = 4$ (squares). Lines are guides to the eye.

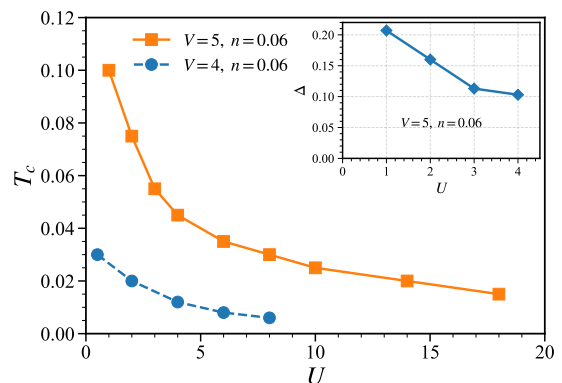


FIG. 4. **Main panel:** Transition temperature T_c as a function of the on-site Coulomb interaction U at two values of inter-orbital interaction V . Squares correspond to $V = 5$, while diamonds correspond to $V = 4$. Here $n_e = n_h = n = 0.06$, and 1×2 - site CDMFT is used. **Inset:** Exciton gap Δ as functions of U at $V = 5$, $n = 0.06$. It should be noted that here Δ is evaluated at a small but finite temperature $T = 0.01$, by using the maximum entropy analytical continuation.

reliably capture the exciton physics.

We now focus on the dependence of critical temperature T_c on the inter-orbital electron-hole attraction V . In Fig. 3, results of T_c as a function of V are shown, where calculations are performed at a fixed electron-hole density $n = 0.06$, and two on-site repulsions $U = 0, U = 4$. In the absence of on-site repulsion ($U = 0$), T_c increases from $T_c \approx 0.006$ to $T_c \approx 0.12$ as V is increased from $V = 3$ to $V = 5$. For the finite U case ($U = 4$), T_c grows from $T_c \approx 0.012$ to $T_c \approx 0.1$ as V increases from $V = 4$ to $V = 6$. At given V , T_c is consistently smaller for $U = 4$ than for $U = 0$, indicating on-site U plays a detrimental role in excitonic condensation.

To systematically investigate the effect of on-site Hubbard repulsion U on excitonic condensation, we computed T_c across a wide range of U values. As shown in FIG. 4, T_c decreases substantially as U increased from zero. This decreasing trend is particularly rapid at smaller U and becomes more gradual for larger U , see both curves in FIG. 4. Specifically, at fixed $V = 5$, increasing U from $U = 1$ to $U = 18$ reduces T_c from $T_c = 0.1$ to $T_c = 0.015$, a decrease by nearly a factor of seven. Similarly, for $V = 4$, raising U from $U = 0.5$ to $U = 12$ lowers T_c from $T_c = 0.03$ to $T_c = 0.005$, corresponding to a sixfold reduction. These results confirm that the on-site repulsion U is a key factor limiting the stability of the excitonic condensed phase in the system. In the inset of Fig. 4, we present the exciton gap Δ as a function of U for $V = 5$ and $n = 0.06$. This gap is extracted from the single-particle gap in the spectral function $A(k, \omega)$ within the exciton condensed phase (see also the Supplementary Information). We observe that Δ is also strongly suppressed by U , following a trend similar to that of T_c as a function of U . This finding

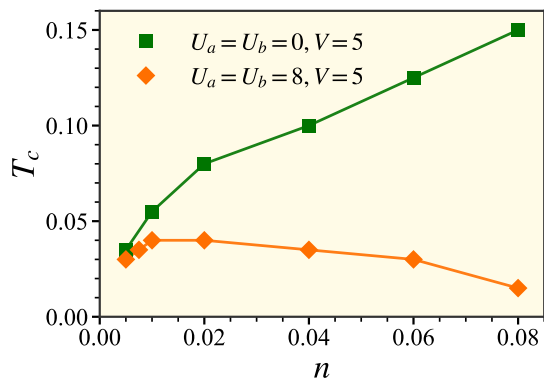


FIG. 5. Transition temperature T_c as a function of the electron-hole density at two different values of U . The inter-orbital interaction is fixed at $V = 5$. 1×2 -site CDMFT is used here.

indicates that in our study, the strong suppression of T_c by U primarily stems from a reduction in the exciton gap, rather than a decrease in the phase stiffness of the excitonic condensate.

Now we investigate the interplay between the on-site repulsion U and the electron-hole density. The density dependence of T_c for $U = 0$ and $U = 8$ is shown in FIG. 5. For the $U = 0$ case ($U = 0, V = 5$), T_c exhibits a monotonic increase from $T_c = 0.035$ to $T_c = 0.15$ as density increases from $n = 0.005$ to $n = 0.08$, indicating that a larger population of charge carriers boosts condensation. In stark contrast, a finite on-site repulsion fundamentally alters this behavior. In the low-density regime ($0.005 < n < 0.01$), T_c exhibits an initial increase for the $U = 8, V = 5$ case (diamonds in FIG. 5), rising from $T_c = 0.03$ to $T_c = 0.04$. As the density increases beyond $n = 0.01$, however, T_c begins to decrease continuously, dropping significantly from $T_c = 0.04$ to $T_c = 0.015$ as n increased from $n = 0.01$ to $n = 0.08$. This non-monotonic trend at finite U reflects a competition between mechanisms. At extremely low carrier density n , on-site repulsion U plays a minor role, increasing n enhances the coherence of electron-hole pairs, leading to higher T_c . When n becomes significantly large, on-site repulsion U tends to dynamically bind intra-orbital local electron-hole pairs. These dynamically generated intra-orbital local electron-hole pairs have a short lifetime due to intra-orbital electron-hole recombination governed by intra-layer hopping t_a and t_b , which prevents them from forming an intra-layer excitonic condensate. Nevertheless, they can compete with the formation of inter-orbital excitons, thereby reducing T_c .

In essence, these results show that in a system where low-energy physics is dominated by d -electrons, the formation of indirect excitons faces significant competition from intra-orbital electron-hole binding. Consequently, the system's low-energy physics is not governed purely by inter-orbital (or inter-layer) excitonic degrees of free-

dom. A theoretical approach that consider only inter-orbital electron-hole binding may therefore miss a key physical ingredient and severely overestimate the phase transition temperature T_c . It is worthy to note that within a pure mean-field treatment (without magnetic symmetry breaking), on-site Hubbard U merely introduces a Hartree shift and does not affect T_c for a given electron-hole density. When further considering quasiparticle renormalization due to U , the dimensionless coupling constant $\tilde{\lambda} = ZVN(0)$ and effective bandwidth $\tilde{W} = ZW$ are renormalized by quasiparticle residue Z , where $N(0)$ is the density of states at the Fermi level. This renormalization does lead to a U -dependent suppression of T_c in mean-field theory. However, at low densities ($n \ll 0.5$) studied here, we find that $Z \sim 1$. Therefore, the observed strong suppression of T_c by U should be attributed to dynamical effects beyond a static mean-field treatment.

Above we have studied the two-orbital electron-hole model. In materials, carriers near Fermi level can also originate from multiple d -orbitals, or from a hybridization with p -orbitals (which possess a smaller on-site U). For instance, in $\text{Ta}_2\text{Pd}_3\text{Te}_5$ [21], hole bands acquire weight from both the Pd- d_{xy} -orbital and Te- p_x -orbital. In Ta_2NiSe_5 , multiple Ta and Ni d -orbitals contribute to the relevant electron and hole bands [80]. This multiplicity of active orbitals can potentially give rise to several distinct channels for electron-hole pair condensation [56], which may compete with one another. To explore the interplay between multiple pairing channels involving d - or p -orbital degrees of freedom, we extend our analysis to a minimal three-orbital model [81–83]. Without loss of generality, we consider a system comprising one electron-type orbital (orbital- a) and two hole-type orbitals (orbital- b, c). In this system, an electron can, in principle, form a bound pair with a hole from either of the other two orbitals, defining two distinct pairing channels (ab -, or ac - channel).

We first examine the case where all three orbitals are of d -electrons, thus large on-site U for all three orbitals shall be assumed. Here the influence of the additional d -hole orbital (orbital- c) is activated by gradually increasing its inter-orbital interaction strength, defined as $V_p \equiv V_{ac} = V_{bc}$ from zero. Simply speaking, when $V_p = 0$, the additional hole orbital- c is fully decoupled from the system, and when $V_p = V_{ab}$, both hole orbitals are equally coupled to the electron orbital. The corresponding evolution of the critical temperature T_c as a function of V_p is shown in Fig. 6(a), where $U_a = U_b = U_c = 4$, and $V_{ab} = 5$ is fixed. As V_p increased from zero, T_c initially remains nearly constant for $V_p \lesssim 2$, forming a plateau. Further increasing V_p then leads to significant suppression of T_c . At $V_p = 5$, namely, when inter-orbital interactions between three orbitals are equal, $V_{ab} = V_{bc} = V_{ac}$, the critical temperature is reduced to $T_c \approx 0.015$, a value slightly exceeding one-third

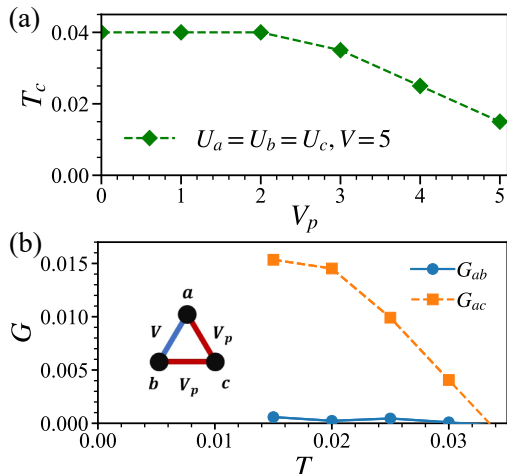


FIG. 6. (a) Transition temperature T_c as a function of inter-orbital $d-d$ Coulomb interaction V_p . Here $n = 0.06$, $U_a = U_b = U_c = 4$, and $V = 5$. (b) **Main panel:** Temperature dependence of the inter-orbital excitonic condensation order parameter G_{ab} (dots) and G_{ac} (squares) in the three-orbital model. Lines are guides for the eye. **Inset (left):** Schematic of the three-orbital model, where the a , b , c are distinct orbital indices. The additional orbital c represents the p -orbital, while a and b represent the d -orbitals. The inter-orbital interaction between orbital c and orbitals a and b is denoted by V_p . Electrons in one orbital can pair with holes in the other two orbitals, and a competition exists between the two types of pairing. Here, $U_a = U_b = 4$, $U_c = 2$, $V = V_p = 5$. 1×2 -site CDMFT is used here.

of that at $V_p = 0$. This strong suppression of T_c upon introducing an additional pairing channel indicates that the competition between pairing channels, *i.e.*, pairing between ab -, or ac - channels, plays a crucial detrimental role in the spontaneous formation of long-range excitonic order. This effect bears a conceptual resemblance to geometric frustration in magnetic systems, where competing magnetic couplings can prevent the establishment of long-range magnetic order, as seen in quantum spin liquids [84]. Here, an analogous “frustration” arises from the presence of multiple, near-degenerate electron-hole pairing channels, which suppresses the excitonic condensation. A key distinction, however, is that in the present case, long-range excitonic order persists even at the maximally frustrated point ($V_{ab} = V_{ac} = V_{bc}$), albeit with a significantly reduced T_c .

We then investigate the scenario with two d -orbitals and one p -orbital: a “strong U ” electron orbital (orbital- a) and a “strong U ” hole orbital (orbital- b) represent the d -orbitals, while a “weak U ” hole orbital (orbital- c) represents the p -orbital. For simplicity, all inter-orbital interactions V are set equal, $V_{ab} = V_{ac} = V_{bc}$. Fig. 6(b) presents the temperature dependence of the excitonic condensation order parameters $G_{mn} = \sum_{\sigma} \langle c_{im\sigma}^{\dagger} c_{in\sigma} \rangle$, for $(m, n) = (a, b), (a, c)$, for parameters $U_a = U_b = 4$, $U_c = 2$, and $V = 5$ in this system. The results re-

veal a remarkable orbital-selective electron-hole pairing phenomenon. Upon cooling, an excitonic order parameter between the d - p orbitals (G_{ac}) emerges spontaneously below a critical temperature of $T_c \approx 0.032t$, and grows with further decreasing T . In contrast, the order parameter between two d - d orbitals (G_{ab}) remains negligible at all temperatures, despite the symmetric inter-orbital attraction ($V_{ab} = V_{ac} = V_{bc}$). This orbital-selective excitonic condensation that prefers a d - p condensation over a d - d condensation likely stems from the effect of Hubbard U , which hinders inter-orbital exciton formation. The p -orbital, with its smaller U , is more susceptible to inter-orbital electron-hole binding than a d -orbital with a larger U . Consequently, the competition between multiple channels is resolved in favor of d - p exciton condensation, resulting in paired states between d - p orbitals and unpaired states between the d - d orbitals.

Discussion and conclusion - In exciton insulator candidate comprising transition metal atoms, such as $\text{Ta}_2\text{Pd}_3\text{Te}_5$ and Ta_2NiSe_5 , electrons and holes are subject to multiple sources of Coulomb attractions. These multiple electron-hole binding routes effectively introduce a “frustration” effect that hinders the formation of exciton condensation. Notably, the on-site Hubbard interaction U , typically the largest energy scale in such systems, can facilitate the formation of local electron-hole pairs or local moments, thereby substantially suppressing the condensation temperature T_c . While our calculations are performed for semimetallic systems with finite carrier densities in the conduction and valence bands, our conclusions should, in principle, remain valid in the semiconductor limit. In actual semiconductors, although the valence band is completely filled and the conduction band empty, orbital hybridization [21], from the local atomic orbital perspective, inevitably generates holes in the valence orbit and electrons in the conduction orbital, ensuring that the suppression of T_c by on-site Hubbard U persists.

In connection with experiments, we note that for TMC excitonic insulator candidates such as $\text{Ta}_2\text{Pd}_3\text{Te}_5$ and Ta_2NiSe_5 , the typical hopping integral is estimated to be $t \approx 0.1 \sim 0.2\text{eV}$ [10]. The screened on-site Hubbard repulsion U for these localized d -orbitals typically spans $U \approx 0.8 \sim 2.5\text{eV}$, while the inter-orbital interaction V is on the order of $V \approx 1.0\text{eV}$ [56, 69]. These physical energy scales yield dimensionless interaction ratios of $U/t \approx 4 \sim 25$ and $V/t \approx 5 \sim 10$, which fall within our simulated parameter space. Based on this mapping, our calculated maximum transition temperature $T_c \approx 0.06t$ at typical parameters ($U = 8t$, $V = 6t$) corresponds to a physical temperature of approximately $70 \sim 140\text{K}$, which is consistent with the experimentally observed $T_c \sim 100\text{K}$ in $\text{Ta}_2\text{Pd}_3\text{Te}_5$ [11].

This agreement suggests that the strong suppression of T_c by on-site Hubbard U , as revealed in our study, may play an important role in resolving the apparent

paradox between the large exciton binding energy and the low condensation temperature observed experimentally. For example, theoretical studies have predicted a large exciton binding energy $\Delta \geq 0.6\text{eV}$ [21] for $\text{Ta}_2\text{Pd}_3\text{Te}_5$, contrasting with its $T_c \sim 100\text{K}$, *i.e.* $k_B T_c \sim 0.01\text{eV}$. This also offers insight into why exciton insulators remain so difficult to detect experimentally, despite the fact that exciton binding energies can be on the order of $\sim 1\text{eV}$ in low-dimensional materials [66–68].

We propose to verify the competing mechanisms in future experiments detecting excitonic condensation temperature T_c versus carrier concentration n , where non-monotonic evolution may be found. On the other hand, with the polarization-dependent angle-resolved photoemission spectroscopy (ARPES) [85–87], future experiments should be able to resolve the orbital differences of the excitonic condensation in multi-orbital excitonic insulator materials, thereby providing an approach to verify the results obtained in this work.

In summary, we have systematically investigated spatially indirect exciton condensation in the two-dimensional Hubbard model on a triangular lattice using dynamical mean-field theory. Our results show that the critical temperature T_c for exciton condensation can be strongly suppressed by intra-orbital Coulomb repulsion U of the d -orbitals. We uncover a remarkable contrast in the density dependence of T_c between $U = 0$ and $U \neq 0$ cases. Extending our analysis to a three-orbital model, we further identify an orbital-selective electron-hole pairing state. These findings indicate that competition among multiple pairing channels in exciton insulator systems can significantly reduce T_c even in the presence of a large exciton binding energy. Our results illuminate the intricate interplay among Coulomb interactions, carrier density, and orbital degrees of freedom, providing valuable theoretical insights into the behavior of excitonic insulators in strongly correlated materials.

Acknowledgment We thank Sheng Chen from the joint Ph.D. program of Sun Yat-sen University and Great Bay University, for useful discussions. This work is supported by the National Natural Science Foundation of China (Grants No.12274472, No.12494594). We also thank the support from the Research Center for Magnetoelectric Physics of Guangdong Province (Grants No.2024B0303390001) and Guangdong Provincial Quantum Science Strategic Initiative (Grant No.GDZX2401010).

* Corresponding author: wuwei69@mail.sysu.edu.cn

- [1] N. F. Mott, The transition to the metallic state, *Philosophical Magazine* **6**, 287 (1961).
- [2] J. M. Blatt, K. Böer, and W. Brandt, Bose-Einstein condensation of excitons, *Physical Review* **126**, 1691 (1962).
- [3] D. Jerome, T. Rice, and W. Kohn, Excitonic insulator, *Physical Review* **158**, 462 (1967).
- [4] J. Eisenstein and A. H. MacDonald, Bose–Einstein condensation of excitons in bilayer electron systems, *Nature* **432**, 691 (2004).
- [5] H. Cercellier, C. Monney, F. Clerc, C. Battaglia, L. Despont, M. G. Garnier, H. Beck, P. Aebi, L. Patthey, H. Berger, and L. Forró, Evidence for an excitonic insulator phase in $1T\text{-TiSe}_2$, *Phys. Rev. Lett.* **99**, 146403 (2007).
- [6] Z. Jiang, Y. Li, W. Duan, and S. Zhang, Half-excitonic insulator: A single-spin Bose-Einstein condensate, *Phys. Rev. Lett.* **122**, 236402 (2019).
- [7] L. Ma, P. X. Nguyen, Z. Wang, Y. Zeng, K. Watanabe, T. Taniguchi, A. H. MacDonald, K. F. Mak, and J. Shan, Strongly correlated excitonic insulator in atomic double layers, *Nature* **598**, 585 (2021).
- [8] E. Baldini, A. Zong, D. Choi, C. Lee, M. H. Michael, L. Windgatter, I. I. Mazin, S. Latini, D. Azoury, B. Lv, *et al.*, The spontaneous symmetry breaking in Ta_2NiSe_5 is structural in nature, *Proceedings of the National Academy of Sciences* **120**, e2221688120 (2023).
- [9] P. Zhang, Y. Dong, D. Yan, B. Jiang, T. Yang, J. Li, Z. Guo, Y. Huang, Haobo, Q. Li, *et al.*, Spontaneous gap opening and potential excitonic states in an ideal dirac semimetal $\text{Ta}_2\text{Pd}_3\text{Te}_5$, *Physical Review X* **14**, 011047 (2024).
- [10] J. Huang, B. Jiang, J. Yao, D. Yan, X. Lei, J. Gao, Z. Guo, F. Jin, Y. Li, Z. Yuan, C. Chai, H. Sheng, M. Pan, F. Chen, J. Liu, S. Gao, G. Qu, B. Liu, Z. Jiang, Z. Liu, X. Ma, S. Zhou, Y. Huang, C. Yun, Q. Zhang, S. Li, S. Jin, H. Ding, J. Shen, D. Su, Y. Shi, Z. Wang, and T. Qian, Evidence for an excitonic insulator state in $\text{Ta}_2\text{Pd}_3\text{Te}_5$, *Phys. Rev. X* **14**, 011046 (2024).
- [11] M. S. Hossain, Z.-J. Cheng, Y.-X. Jiang, T. A. Cochran, S.-B. Zhang, H. Wu, X. Liu, X. Zheng, G. Cheng, B. Kim, *et al.*, Topological excitonic insulator with tunable momentum order, *Nature Physics* **21**, 1250 (2025).
- [12] Q. Gao, Y.-h. Chan, P. Jiao, H. Chen, S. Yin, K. Tangphapha, Y. Yang, X. Li, Z. Liu, D. Shen, *et al.*, Observation of possible excitonic charge density waves and metal–insulator transitions in atomically thin semimetals, *Nature Physics* **20**, 597 (2024).
- [13] Q. Wang, G. Xue, C. Ji, Y. Li, C. Li, L. Hou, X. Zheng, Q. Yu, C. Ma, X. Gan, *et al.*, Resonance tuning of localized excitons via a plasmonic nanocavity, *ACS nano* (2026).
- [14] Y. Meng and Z. Wang, Isolating and identification of layer dependence of correlated states in $\text{MoSe}_2/\text{WS}_2$ moiré heterojunction, *Science China Physics, Mechanics & Astronomy* **68**, 267811 (2025).
- [15] X. Liu, S. Liu, Y. Xiao, C. Xu, J. Wu, K. Li, S.-Y. Li, and A. Pan, Probing the special angle in twisted bilayer MoS_2 via angle-dependent scanning tunneling microscopy studies, *Science China Physics, Mechanics & Astronomy* **68**, 226811 (2025).
- [16] Y. E. Lozovik and V. Yudson, A new mechanism for superconductivity: pairing between spatially separated electrons and holes, *Zh. Eksp. Teor. Fiz* **71**, 738 (1976).
- [17] F.-C. Wu, F. Xue, and A. H. MacDonald, Theory of two-dimensional spatially indirect equilibrium exciton condensates, *Phys. Rev. B* **92**, 165121 (2015).
- [18] Z. Jiang, Z. Liu, Y. Li, and W. Duan, Scaling universality between band gap and exciton binding energy of two-dimensional semiconductors, *Phys. Rev. Lett.* **118**,

- 266401 (2017).
- [19] M. Guan, D. Chen, Q. Chen, Y. Yao, and S. Meng, Coherent phonon assisted ultrafast order-parameter reversal and hidden metallic state in Ta_2NiSe_5 , *Phys. Rev. Lett.* **131**, 256503 (2023).
- [20] Y. Shao and X. Dai, Electrical breakdown of excitonic insulators, *Phys. Rev. X* **14**, 021047 (2024).
- [21] J. Yao, H. Sheng, R. Zhang, R. Pang, J.-J. Zhou, Q. Wu, H. Weng, X. Dai, Z. Fang, and Z. Wang, Excitonic instability in $\text{Ta}_2\text{Pd}_3\text{Te}_5$ monolayer, *Chinese Physics Letters* **41**, 097101 (2024).
- [22] Y. Zeng, A. H. MacDonald, and N. Wei, Topological excitonic insulators in electron bilayers modulated by twisted hBN, *arXiv preprint arXiv:2509.11041* (2025).
- [23] Y. Xia, L. Shu, Y. Zhang, Y. Chen, L. Peng, J. Zhang, B. Li, H. Shao, Y. Cen, Z. Sui, *et al.*, Full-landscape condensation phases for long-lived excitons in 2d tellurium: Crystal-field splitting and finite-momentum excitons, *Advanced Functional Materials* **33**, 2303779 (2023).
- [24] G. Sreejith, J. D. Sau, and S. Das Sarma, Eliashberg theory for dynamical screening in bilayer exciton condensation, *Physical Review Letters* **133**, 056501 (2024).
- [25] S. Giuli, A. Amaricci, and M. Capone, Mott-enhanced exciton condensation in a Hubbard bilayer, *Physical Review B* **108**, 165150 (2023).
- [26] J.-X. Zhu and A. Bishop, Exciton condensate modulation in electron-hole bilayers: A real-space visualization, *Physical Review B—Condensed Matter and Materials Physics* **81**, 115329 (2010).
- [27] J. Zhu and S. Das Sarma, Interaction and coherence in two-dimensional bilayers, *Physical Review B* **109**, 085129 (2024).
- [28] P. López Ríos, A. Perali, R. J. Needs, and D. Neilson, Evidence from quantum monte carlo simulations of large-gap superfluidity and BCS-BEC crossover in double electron-hole layers, *Physical Review Letters* **120**, 177701 (2018).
- [29] F. Nilsson and F. Aryasetiawan, Effects of dynamical screening on the BCS-BEC crossover in double bilayer graphene: Density functional theory for exciton bilayers, *Physical Review Materials* **5**, L050801 (2021).
- [30] B. H. Moon, A. Mondal, D. K. Efimkin, and Y. H. Lee, Exciton condensate in van der Waals layered materials, *Nature Reviews Physics* , 1 (2025).
- [31] Q. Gao, Y.-h. Chan, Y. Wang, H. Zhang, P. Jinxi, S. Cui, Y. Yang, Z. Liu, D. Shen, Z. Sun, *et al.*, Evidence of high-temperature exciton condensation in a two-dimensional semimetal, *Nature Communications* **14**, 994 (2023).
- [32] Z. Wang, D. A. Rhodes, K. Watanabe, T. Taniguchi, J. C. Hone, J. Shan, and K. F. Mak, Evidence of high-temperature exciton condensation in two-dimensional atomic double layers, *Nature* **574**, 76 (2019).
- [33] S. Conti, A. Perali, A. R. Hamilton, M. V. Milošević, F. m. c. M. Peeters, and D. Neilson, Chester supersolid of spatially indirect excitons in double-layer semiconductor heterostructures, *Phys. Rev. Lett.* **130**, 057001 (2023).
- [34] Y.-H. Zhang, D. N. Sheng, and A. Vishwanath, $\text{SU}(4)$ chiral spin liquid, exciton supersolid, and electric detection in moiré bilayers, *Phys. Rev. Lett.* **127**, 247701 (2021).
- [35] D. D. Dai and L. Fu, Strong-coupling phases of trions and excitons in electron-hole bilayers at commensurate densities, *Phys. Rev. Lett.* **132**, 196202 (2024).
- [36] X. Chen and J. Quinn, Excitonic charge-density-wave instability of spatially separated electron-hole layers in strong magnetic fields, *Physical review letters* **67**, 895 (1991).
- [37] Z. Bi and L. Fu, Excitonic density wave and spin-valley superfluid in bilayer transition metal dichalcogenide, *Nature communications* **12**, 642 (2021).
- [38] Y. Zeng, Z. Xia, R. Dery, K. Watanabe, T. Taniguchi, J. Shan, and K. F. Mak, Exciton density waves in Coulomb-coupled dual moiré lattices, *Nature Materials* **22**, 175 (2023).
- [39] S. Dong, Y. Chen, H. Qu, W.-K. Lou, and K. Chang, Topological exciton density wave in monolayer WSe_2 , *Phys. Rev. Lett.* **134**, 066602 (2025).
- [40] R. Wang, T. A. Sedrakyan, B. Wang, L. Du, and R.-R. Du, Excitonic topological order in imbalanced electron-hole bilayers, *Nature* **619**, 57 (2023).
- [41] P. X. Nguyen, L. Ma, R. Chaturvedi, K. Watanabe, T. Taniguchi, J. Shan, and K. F. Mak, Perfect Coulomb drag in a dipolar excitonic insulator, *Science* **388**, 274 (2025).
- [42] R. Qi, A. Y. Joe, Z. Zhang, J. Xie, Q. Feng, Z. Lu, Z. Wang, T. Taniguchi, K. Watanabe, S. Tongay, *et al.*, Perfect Coulomb drag and exciton transport in an excitonic insulator, *Science* **388**, 278 (2025).
- [43] X. Zhu, P. B. Littlewood, M. S. Hybertsen, and T. M. Rice, Exciton condensate in semiconductor quantum well structures, *Phys. Rev. Lett.* **74**, 1633 (1995).
- [44] D. Snoke, Spontaneous bose coherence of excitons and polaritons, *Science* **298**, 1368 (2002).
- [45] K. Ulman and S. Y. Quek, Organic-2D material heterostructures: A promising platform for exciton condensation and multiplication, *Nano Letters* **21**, 8888 (2021).
- [46] E. C. Regan, D. Wang, E. Y. Paik, Y. Zeng, L. Zhang, J. Zhu, A. H. MacDonald, H. Deng, and F. Wang, Emerging exciton physics in transition metal dichalcogenide heterobilayers, *Nature Reviews Materials* **7**, 778 (2022).
- [47] D. Nandi, A. Finck, J. Eisenstein, L. Pfeiffer, and K. West, Exciton condensation and perfect Coulomb drag, *Nature* **488**, 481 (2012).
- [48] J. A. Seamons, C. P. Morath, J. L. Reno, and M. P. Lilly, Coulomb Drag in the Exciton Regime in Electron-Hole Bilayers, *Phys. Rev. Lett.* **102**, 026804 (2009).
- [49] A. Kogar, M. S. Rak, S. Vig, A. A. Husain, F. Flicker, Y. I. Joe, L. Venema, G. J. MacDougall, T. C. Chiang, E. Fradkin, *et al.*, Signatures of exciton condensation in a transition metal dichalcogenide, *Science* **358**, 1314 (2017).
- [50] Y. Ou, L. Chen, Z. Xin, Y. Ren, P. Yuan, Z. Wang, Y. Zhu, J. Chen, and Y. Zhang, Incoherence-to-coherence crossover observed in charge-density-wave material $1T\text{-TiSe}_2$, *Nature Communications* **15**, 9202 (2024).
- [51] X.-Q. Ye, H. Liu, Q.-Y. Wu, C. Zhang, X.-F. Tang, B. Chen, C.-C. Shu, H.-Y. Liu, Y.-X. Duan, P. M. Oppeneer, *et al.*, Ultrafast phonon hardening and nonthermal lattice potential reconstruction in the charge-density-wave material $1T\text{-TiSe}_2$, *Science China Physics, Mechanics & Astronomy* **69**, 267412 (2026).
- [52] H. Yu, D. Yan, Z. Guo, Y. Zhou, X. Yang, P. Li, Z. Wang, X. Xiang, J. Li, X. Ma, R. Zhou, F. Hong, Y. Wuli, Y. Shi, J.-T. Wang, and X. Yu, Observation of emergent superconductivity in the topological insulator $\text{Ta}_2\text{Pd}_3\text{Te}_5$ via pressure manipulation, *Journal of the American Chemical Society* **146**, 3890 (2024), pMID: 38294957, <https://doi.org/10.1021/jacs.3c11364>.

- [53] S. Bae, A. Raghavan, I. Feldman, A. Kanigel, and V. Madhavan, Microscopic evidence of dominant excitonic instability in Ta_2NiSe_5 , [arXiv preprint arXiv:2512.03011 \(2025\)](#).
- [54] C. Chen, X. Chen, W. Tang, Z. Li, S. Wang, S. Ding, Z. Kang, C. Jozwiak, A. Bostwick, E. Rotenberg, M. Hashimoto, D. Lu, J. P. C. Ruff, S. G. Louie, R. J. Birgeneau, Y. Chen, Y. Wang, and Y. He, Role of electron-phonon coupling in excitonic insulator candidate Ta_2NiSe_5 , [Phys. Rev. Res.](#) **5**, 043089 (2023).
- [55] T. Li, Y. Liu, H. Zhu, H. Chen, Z. Liu, Z. Shang, Y. Li, H. Tian, Y. Wu, Y. Hong, *et al.*, Disentangling the electron-lattice dichotomy of the excitonic insulating phase in $\text{Ta}_2\text{Ni}(\text{Se}_{1-x}\text{S}_x)_5$ with sulfur substitution and potassium deposition, [Science China Physics, Mechanics & Astronomy](#) **67**, 126811 (2024).
- [56] G. Mazza, M. Rösner, L. Windgätter, S. Latini, H. Hübener, A. J. Millis, A. Rubio, and A. Georges, Nature of symmetry breaking at the excitonic insulator transition: Ta_2NiSe_5 , [Phys. Rev. Lett.](#) **124**, 197601 (2020).
- [57] Q. Liu, D. d. Wu, Z. Li, L. Shi, Z. Wang, S. Zhang, T. Lin, T. Hu, H. Tian, J. Li, *et al.*, Photoinduced multistage phase transitions in Ta_2NiSe_5 , [Nature Communications](#) **12**, 2050 (2021).
- [58] K. Wei, Y. Luo, K. Watanabe, T. Taniguchi, Y. Guo, and X. Xi, Gate tuning of coupled electronic and structural phase transition in atomically thin Ta_2NiSe_5 , [Nature Communications](#) **16**, 10999 (2025).
- [59] Z. Chen, C. Xu, C. Xie, W. Tang, Q. Liu, D. Wu, Q. Xu, T. Jiang, P. Zhu, X. Zou, *et al.*, Structural contribution to light-induced gap suppression in Ta_2NiSe_5 , [Physical Review Letters](#) **135**, 096901 (2025).
- [60] K. Kim, H. Kim, J. Kim, C. Kwon, J. S. Kim, and B. Kim, Direct observation of excitonic instability in Ta_2NiSe_5 , [Nature communications](#) **12**, 1969 (2021).
- [61] A. Kozlov and L. Maksimov, The metal-dielectric divalent crystal phase transition, [Sov. Phys. JETP](#) **21**, 790 (1965).
- [62] F. X. Bronold and H. Fehske, Possibility of an excitonic insulator at the semiconductor-semimetal transition, [Physical Review B—Condensed Matter and Materials Physics](#) **74**, 165107 (2006).
- [63] M. Fogler, L. Butov, and K. Novoselov, High-temperature superfluidity with indirect excitons in van der waals heterostructures, [Nature communications](#) **5**, 4555 (2014).
- [64] M. Combescot, R. Combescot, and F. Dubin, Bose-Einstein condensation and indirect excitons: a review, [Reports on Progress in Physics](#) **80**, 066501 (2017).
- [65] T. Kaneko and Y. Ohta, A new era of excitonic insulators, [Journal of the Physical Society of Japan](#) **94**, 012001 (2025).
- [66] H. Tang, L. Yin, G. I. Csonka, and A. Ruzsinszky, Exploring the exciton insulator state in $1T\text{-TiSe}_2$ monolayer with advanced electronic structure methods, [Phys. Rev. B](#) **111**, L201401 (2025).
- [67] Y. Zhao, H. Qu, J. Zhao, L. Kang, and S. Zhou, One-dimensional excitonic insulator of M_6Te_6 ($\text{M} = \text{Mo}, \text{W}$) atomic wires, [Nano Letters](#) **25**, 1108 (2025).
- [68] D. Sun, Y. Xu, L.-A. Qin, Y. Dai, B. Huang, Z. Qian, R. Ahuja, and W. Wei, Breaking the synergy between the quasiparticle band gap and exciton binding energy, bright-dark exciton transition, and realization of the excitonic insulator state in quantum spin hall insulators, [Nano Letters](#) **25**, 18117 (2025).
- [69] H. R. Ramezani, E. Şaşıoğlu, H. Hadipour, H. R. Soleimani, C. Friedrich, S. Blügel, and I. Mertig, Non-conventional screening of Coulomb interaction in two-dimensional semiconductors and metals: A comprehensive constrained random phase approximation study of MX_2 ($\text{M} = \text{Mo}, \text{W}, \text{Nb}, \text{Ta}; \text{X} = \text{S}, \text{Se}, \text{Te}$), [Physical Review B](#) **109**, 125108 (2024).
- [70] A. Georges, G. Kotliar, W. Krauth, and M. J. Rozenberg, Dynamical mean-field theory of strongly correlated fermion systems and the limit of infinite dimensions, [Rev. Mod. Phys.](#) **68**, 13 (1996).
- [71] R. Blankenbecler, D. Scalapino, and R. Sugar, Monte carlo calculations of coupled boson-fermion systems. i, [Physical Review D](#) **24**, 2278 (1981).
- [72] J. Kuneš, Excitonic condensation in systems of strongly correlated electrons, [Journal of Physics: Condensed Matter](#) **27**, 333201 (2015).
- [73] T. Kaneko, K. Seki, and Y. Ohta, Excitonic insulator state in the two-orbital hubbard model: Variational cluster approach, [Phys. Rev. B](#) **85**, 165135 (2012).
- [74] J. Kuneš and P. Augustinský, Excitonic instability at the spin-state transition in the two-band hubbard model, [Phys. Rev. B](#) **89**, 115134 (2014).
- [75] P. Seth, I. Krivenko, M. Ferrero, and O. Parcollet, TRIQS/CTHYB: A continuous-time quantum monte carlo hybridisation expansion solver for quantum impurity problems, [Computer Physics Communications](#) **200**, 274 (2016).
- [76] O. Parcollet, M. Ferrero, T. Ayral, H. Hafermann, I. Krivenko, L. Messio, and P. Seth, TRIQS: A toolbox for research on interacting quantum systems, [Computer Physics Communications](#) **196**, 398–415 (2015).
- [77] T. Wang, S. Miao, Z. Li, Y. Meng, Z. Lu, Z. Lian, M. Blei, T. Taniguchi, K. Watanabe, S. Tongay, *et al.*, Giant valley-zeeman splitting from spin-singlet and spin-triplet interlayer excitons in $\text{WSe}_2/\text{MoSe}_2$ heterostructure, [Nano letters](#) **20**, 694 (2019).
- [78] Y. Li, Z. Yan, and S. Wang, Spin character of interlayer excitons in tungsten dichalcogenide heterostructures: GW-BSE calculations, [Physical Review B](#) **109**, 045422 (2024).
- [79] M. A. Durmuş and I. Sarpkaya, Quantum beats between spin-singlet and spin-triplet interlayer exciton transitions in $\text{WSe}_2\text{-MoSe}_2$ heterobilayers, [Nano Letters](#) **24**, 5767 (2024).
- [80] X. Ma, G. Wang, H. Mao, Z. Yuan, T. Yu, R. Liu, Y. Peng, P. Zheng, and Z. Yin, Ta_2NiSe_5 : A candidate topological excitonic insulator with multiple band inversions, [Phys. Rev. B](#) **105**, 035138 (2022).
- [81] E. Cappelluti, R. Roldán, J. Silva-Guillén, P. Ordejón, and F. Guinea, Tight-binding model and direct-gap/indirect-gap transition in single-layer and multilayer MoS_2 , [Physical Review B—Condensed Matter and Materials Physics](#) **88**, 075409 (2013).
- [82] Z. Y. Zhu, Y. C. Cheng, and U. Schwingenschlögl, Giant spin-orbit-induced spin splitting in two-dimensional transition-metal dichalcogenide semiconductors, [Phys. Rev. B](#) **84**, 153402 (2011).
- [83] G.-B. Liu, W.-Y. Shan, Y. Yao, W. Yao, and D. Xiao, Three-band tight-binding model for monolayers of group-VIB transition metal dichalcogenides, [Physical Review B—Condensed Matter and Materials Physics](#) **88**,

- 085433 (2013).
- [84] Y. Zhou, K. Kanoda, and T.-K. Ng, Quantum spin liquid states, *Reviews of Modern Physics* **89**, 025003 (2017).
- [85] S. Beaulieu, J. Schusser, S. Dong, M. Schüler, T. Pincelli, M. Dendzik, J. Maklar, A. Neef, H. Ebert, K. Hricovini, M. Wolf, J. Braun, L. Rettig, J. Minár, and R. Ernstorfer, Revealing hidden orbital pseudospin texture with time-reversal dichroism in photoelectron angular distributions, *Phys. Rev. Lett.* **125**, 216404 (2020).
- [86] J. A. Sobota, Y. He, and Z.-X. Shen, Angle-resolved photoemission studies of quantum materials, *Rev. Mod. Phys.* **93**, 025006 (2021).
- [87] J. Ma and M. Shi, Angle resolved photoemission spectroscopy study of excitons in quantum materials, *Science China Physics, Mechanics & Astronomy* **68**, 287001 (2025).